Plant mercury pump controls seasonal variations in global atmospheric mercury

Jiskra, Martin[1]; Sonke, Jeroen E.[1]; Obrist, Daniel[2]; Bieser, Johannes;[3] Ebinghaus, Ralf;[3] Myhre, Cathrine Lund[4]; Aspmo, Katrine[4]; Wängberg, Ingvar[5]; Kyllönen, Katriina[6]; Worthy, Doug[7]; Martin, Lynwill G.[8]; Labuschagne Casper[8]; Mkololo, Thumeka[8]; Ramonet, Michel[9]; Magand, Olivier[9]; and Dommergue, Aurélien[9]

[1]Geosciences Environnement Toulouse, CNRS/OMP/Université de Toulouse, 14 Avenue Edouard Belin, 31400 Toulouse, France.
[2]Department of Environmental, Earth, and Atmospheric Sciences, University of Massachusetts, Lowell, MA 01854, USA
[3]Helmholtz Zentrum Geesthacht, Institute of Coastal Research, 21502 Geesthacht, Germany
[4]NILU - Norwegian Institute for Air Research, 2027 Kjeller, Norway
[5]Swedish Environment Institute, 40014 Gothenburg, Sweden
[6]Finnish Meteorological Institute, Atmospheric Composition Research, 00560 Helsinki, Finland
[7]Environment and Climate Change Canada, Climate Research Division, Toronto, Canada
[8]Cape Point GAW Station, South African Weather Service, 11 Jan Cilliers Street, Stellenbosch, South Africa
[9]Univ. Grenoble Alpes, CNRS, IRD, IGE, 38000 Grenoble, France

This is a post print version
DOI to the published version in Nature Geoscience: https://doi.org/10.1038/s41561-018-0078-8

Abstract

Anthropogenic mercury emissions are transported through the atmosphere as gaseous elemental mercury (Hg(0)) prior to deposition to earth surfaces. Two explanations for strong Hg(0) seasonality in the Northern Hemisphere (NH) are variations in primary anthropogenic Hg(0) emissions, thought to peak in winter due to higher energy consumption, and faster atmospheric Hg(0) oxidation rates in summer. Global Hg models simulate equally pronounced, oxidation-driven Hg(0) seasonality in the Southern Hemisphere (SH) where Hg(0) levels are observed to be constant year-round. Furthermore, power consumption related Hg emissions in N-America are higher in summer than in winter, which is inconsistent with low N-American summertime Hg(0) concentrations. Here, we assess the role of Hg(0) uptake by plants as an alternative driving mechanism for global Hg(0) variability. We find that data from all terrestrial background sites in the NH show a co-variation of Hg(0) with CO_2, which is known to exhibit concentration minima in summer due to CO_2 assimilation by vegetation. The amplitude of seasonal Hg(0) oscillations increase with latitude in the NH and are larger at inland terrestrial background sites compared to coastal sites. We find that satellite-derived vegetation photosynthetic activity (NDVI) correlates with Hg(0) levels at individual sites and across continents. These findings suggest vegetation to be a global Hg(0) pump, that dominates seasonal variations of atmospheric Hg(0). We suggest that decreasing Hg(0) levels in the NH over the last 20 years were partly caused by increased Hg(0) uptake by vegetation due to increased terrestrial net primary production.

This is a post print version
DOI to the published version in Nature Geoscience: https://doi.org/10.1038/s41561-018-0078-8

Atmospheric mercury cycling

Gaseous elemental mercury (Hg(0)) is the dominant form of natural and anthropogenic Hg emissions and is transported globally through the atmosphere[1]. Hg deposition to earth surfaces occurs either by direct Hg(0) dry deposition or after oxidation to reactive Hg^{II}, which is scavenged from the atmosphere by wet and dry deposition.[2] In addition to primary anthropogenic emissions, Hg is also re-emitted as Hg(0) from land and ocean surfaces to the atmosphere after reduction of Hg(II) pools in terrestrial and aquatic ecosystems[2].

The short-term balance between Hg emission, deposition and re-emission processes governs diurnal and seasonal Hg(0) variations. For example, strong seasonal variations in atmospheric Hg(0) concentration have been described for most background sites in the temperate Northern Hemisphere (NH) with peaks in winter and minima in summer.[3-6] Two widely accepted hypotheses for the observed Hg(0) seasonality exist. The first hypothesis assumes that Hg(0) variations are directly related to primary anthropogenic Hg(0) emissions from coal combustion which are thought to be higher in winter due to higher energy demands for heating.[3,5] Global Hg models have not yet been able to test this hypothesis, as current anthropogenic Hg emission inventories have no seasonal resolution and are kept constant throughout the year in models.[7-9] The second hypothesis suggests that atmospheric Hg(0) oscilations are due to variations in atmospheric Hg(0) oxidation rate and subsequent Hg(II) deposition which are both highest in summer in global Hg models.[7-10] Models incorporating atmospheric Hg(0) oxidation simulate equally-pronounced (amplitudes of approx. 18%) seasonal Hg(0) variations in both Hemispheres. Hg(0) measurements at temperate sites in the Southern Hemisphere (SH) however are constant with no seasonal oscillations.[6,11] Methane concentrations in the SH, for which atmospheric oxidation by OH radicals represents the most important sink, do show strong seasonal variations.[12] The absence of Hg(0) seasonality in the SH questions the relative importance of atmospheric Hg(0) oxidation.

Foliar uptake of atmospheric Hg(0) has long been recognized as a potentially inportant pathway for atmospheric Hg deposition.[13,14] The magnitude of terrestrial-atmosphere net Hg(0) exchange (foliar Hg(0) uptake - Hg(0) re-emission) however has been debated and most studies suggested a net emission of Hg(0).[15-18] A recent review of Hg(0) flux measurements over terrestrial surfaces concludes that there is no consensus whether terrestrial ecosystems are a net sink or source for Hg(0) (-513 to 1651 Mg a^{-1}, 25 to 75 percentile)[19]. Most Hg(0) flux studies however focused on soil re-emission, and thus neglected foliar Hg(0) exchange.[19]

This is a post print version
DOI to the published version in Nature Geoscience: https://doi.org/10.1038/s41561-018-0078-8

There are several lines of evidence for net Hg(0) deposition to terrestrial ecosystems that all invoke direct plant uptake of atmospheric Hg(0). First, foliage tissue Hg concentrations increase continously over the growing season, implying that Hg(0) is taken up by plants through gas exchange and sequestered in leaf tissue.[14,20] Structurally incorporated Hg in leaf tissue derived from atmospheric Hg(0) therefore likely has a lower re-emission potential due to photo-reduction,[20,21] compared to Hg(II) deposited onto external leaf surfaces.[22] Second, global litterfall Hg deposition to soils - representing Hg(0) net uptake by foliage - is estimated to be 1000-1200 Mg yr^{-1} [17,23] representing half of primary anthropogenic emissions.[24] Third, vegetation and soil Hg stable isotope signatures, which discern foliar Hg(0) uptake from Hg(II) wet deposition, put firm constraints on plant Hg(0) uptake dominating (50-80%) Hg deposition at terrestrial sites. [21,25-27]

Here, we investigate the role of Hg(0) uptake by plants in modulating global atmospheric Hg(0) seasonality. We compare the atmospheric dynamics of Hg(0) with those of CO_2 - a tracer for gas exchange by plants - for which seasonal oscillations in the Northern Hemisphere (NH) are attributed to the balance of CO_2 assimilation and respiration during the year.[28-30]

Correlation of Hg(0) and CO_2 seasonality

We investigated multi-year time series of Hg(0) and CO_2 at seven NH and SH background sites (mean Hg(0) < 2 ng/m^3) and Hg(0) at an additional 43 global sites. Multi-year Hg(0) and CO_2 observations of the five NH background sites, normalized for linear long-term trends, show seasonal variations with highest concentrations in winter and minima in summer and fall (**Fig. 1, S1, S3 and S6**). For all NH sites, we found a significant positive correlation between Hg(0) and CO_2 (Pearson's product-moment correlation of monthly means, normalized for long-term trends, Birkenes, Norway ($r=0.37$, $p<0.005$), Schauinsland, Germany ($r=0.50$, $p<0.001$), Mace Head, Ireland ($r=0.40$, $p<0.001$), Pallas, Finland ($r=0.54$, $p<0.001$) and Egbert, Canada ($r=0.53$, $p<0.001$)). We investigated two coastal SH sites, Cape Point (South Africa) and Amsterdam Island (France), with the latter surrounded by 3000 km of ocean on all sides. Cape Point showed a weaker ($r=0.30$, $p<0.01$) correlation and no clear seasonal variation and Amsterdam Island did not show a significant correlation between the two trace gases. Both SH sites show small day-to-day variability, small diurnal variation and small seasonal amplitudes in CO_2, (<3 ppm, <1%) and Hg(0) (<0.1 ng/m^3, <10%) (**Fig. 1**). This suggests low anthropogenic

This is a post print version
DOI to the published version in Nature Geoscience: https://doi.org/10.1038/s41561-018-0078-8

contributions (i.e., no pollution plumes) as well as atmosphere-ocean exchange of Hg(0) that is relatively constant throughout the day and seasons.

We find that the interhemispheric gradient in Hg(0) concentrations ($\Delta Hg_{45°N-45°S}$) is largest in February (0.66 ng/m^3) and smallest in September (0.43 ng/m^3) with a yearly average of 0.54 ng/m^3 (**Fig 2A**). Two thirds of the primary anthropogenic emissions are to the NH,[31] which is the main explanation for the higher NH Hg(0) concentrations compared to the SH.[6]

The seasonal amplitudes of Hg(0) measurements at temperate NH background sites are much larger, averaging 0.39 ng/m^3 (equivalent to 25% of the average annual Hg(0) concentration of 1.5-1.7 ng/m^3),[6] and were 6 times larger than the corresponding CO_2 amplitudes (4%). Excluding Polar sites (see below), we find a positive correlation (r=0.88, p<0.01, Pearson's product-momentum correlation) between seasonal Hg(0) (Sep-Feb) and CO_2 (Aug-Feb) amplitudes (**Fig. 2C**). Amplitudes of seasonal CO_2 oscillations are largest at high NH latitudes and decrease towards the south with minimal oscillations in the SH, which has been related to varying CO_2 exchange during the vegetation period in the NH, and fewer land masses in the SH.[28-30] We find a significant correlation between the seasonal Hg(0) amplitudes of all background sites (n=38) and latitude (R^2 = 0.42, p<0.001, Figure 2B). However, Hg(0) amplitudes are confounded by additional factors. For example, we explain a lower amplitude of Egbert (Ca) by relatively high contributions of polluted air masses throughout the year (Figure S12). Comparing all investigated sites, we find significantly lower Hg(0) amplitudes at coastal sites compared to inland background sites, both for Europe (0.25 ng/m^3 vs. 0.39 ng/m^3, n=13, p<0.05, 2-sided t-test) and North America (0.27 ng/m^3 vs. 0.41 ng/m^3, n=18, p<0.05, 2-sided t-test). A special case is a different seasonality of Hg(0) in the Arctic, which is typically characterized by spring minima due to sea-salt induced atmospheric mercury depletion events (AMDEs) and an unusual summertime maximum.[32] Observations from SH terrestrial background sites are few, yet the first measurements in Bariloche, Patagonia (Ar) revealed seasonal Hg(0) oscillations with minima in SH summer and autumn.[33]

If seasonal variations in atmospheric Hg(0) were mainly due to oxidation rates and ocean re-emission,[7-9] one would expect higher Hg(0) amplitudes at coastal sites and in the SH, which is contrary to the patterns described above. On an ecosystem scale, studies have reported enhanced Hg deposition fluxes during vegetation growth periods[21,34] and lower local atmospheric Hg(0) levels over vegetated surfaces.[35,26,36] The fact that the highest seasonal amplitudes are observed at inland terrestrial background sites — along with similar patterns

This is a post print version
DOI to the published version in Nature Geoscience: https://doi.org/10.1038/s41561-018-0078-8

observed for CO_2 — argues for a dominant role of vegetation Hg(0) uptake in modulating global atmospheric Hg(0) concentrations. The NH is not only more populated but also has a much larger land mass (68%) compared to the SH (32%), resulting in higher plant Hg(0) uptake which may explain the weaker interhemispheric gradient during the NH growing season.

Most NH sites reveal a remarkable 1-month offset in Hg(0) summertime minima (Sep) compared to CO_2 (Aug) (**Fig. S3, S6**). Opposite oscillation in diurnal Hg(0) and CO_2 concentrations (Fig. S4) and later seasonal minima of Hg(0) relative to CO_2 suggests that Hg(0) uptake by plants is continuing during periods of net CO_2 respiration during nighttime and in fall, when the ecosystem exchange of CO_2 turns from net assimilation to net respiration.[37] Hg(0) thus follows a similar behavior as carbonyl sulfide (COS), for which seasonal patterns are coupled to CO_2, whereas diurnal variations are decoupled.[38,39] This suggests that Hg(0) plant uptake is controlled by plant gas exchange as represented by CO_2 here. Foliar Hg(0) re-emission however is decoupled from CO_2 respiration and is likely limited. This is reflected in increasing Hg concentrations in foliage over the growing season.[13,20,35] The observed Hg(0) concentration minimum in September may be amplified by a shallower planetary boundary layer (PBL) in autumn leading to a reduced mixing with background air.[30]

Variations in Hg(0) vs. vegetation Index

We compared monthly Hg(0) concentrations with the satellite-based Normalized Differenced Vegetation Index (NDVI), representing the vegetation photosynthetic activity and thus a proxy for plant gas exchange, at the location of the 44 NH monitoring sites (0.1° resolution). We find a significant correlation between monthly Hg(0) and and NDVI for for 22 of the 44 investigated sites. For the NH background sites where Hg(0) and CO_2 was measured, NDVI significantly correlated with both trace gases (Fig. 3, Table S1), with the exception of Hg(0) at Schauinsland, De. For example, at Pallas NDVI was able to explain 69 % and 82% of seasonal Hg(0) and CO_2 variation, respectively. The correlation was strongest at background sites in Canada ($R^2 > 0.75$ for e.g. Burnt Island, or Kejimkijuk, Figure S8, Table S2), Scandinavia ($R^2 > 0.6$ for e.g. Andoya, Bredkäle, or Vavihill, Fig. S9, Table S3) or for some Mountain sites in China ($R^2 \approx 0.5$ for e.g. Mt. Damai, Mt. Leigong, Mt. Chanbai, Fig. S10, Table S4). For urban sites in North America (e.g. Salt Lake City, Houston or Detroit, Fig. S7, Table S2) or Asia (Beijing, Nanjing, Fig. S10, Table S4) we did not find a significant correlation between Hg(0) and NDVI (red points in **Fig. S8**), indicating that local anthropogenic emissions dominate Hg(0) levels at urban sites. The

This is a post print version
DOI to the published version in Nature Geoscience: https://doi.org/10.1038/s41561-018-0078-8

relatively strong correlation between Hg(0) concentrations and NDVI at regional background sites suggests that vegetation uptake is responsible for Hg(0) depletion in summer months, when vegetation photosynthetic activity and thus gas exchange of plants is strongest (high NDVI). Note that NDVI is able to describe a higher degree of the Hg(0) variance compared to CO_2 concentrations which we relate to the fact that CO_2 respiration from terrestrial ecosystems is decoupled from Hg(0) re-emission. We therefore suggest that NDVI satellite data might be a robust parameter to estimate terrestrial Hg(0) uptake fluxes on a spatial and temporal scale. Field studies comparing Hg(0) fluxes with vegetation cover are needed in order to validate this approach. A recent study found a strong correlation of soil Hg pools with NDVI across western North America,[40] suggesting a long-term control of the plant Hg(0) pump on soil Hg pools, which is strongly supported by Hg stable isotope data. [21,25-27]

Seasonality of Hg(0) emissions approximated by coal consumption statistics

Coal combustion represents a major primary Hg(0) emission source to the atmosphere.[31] We estimated the seasonal variation of anthropogenic Hg emissions (Table S4) by using monthly coal consumption data reported for the United States, Europe (EU27) and China. The estimates show a peak in Hg emission during the cold winter months attributed to increased energy consumption for heating (**Fig. 4,** Table S4). In North America, there is a second peak in coal consumption and thus Hg(0) emission (**Fig. 4**, Table S4) during hot summer months that exceeds the winter peak and is attributed to high energy consumption for air-conditioning of buildings.[41] Hg(0) concentrations measured at three urban monitoring sites in North America (Salt Lake City, Houston and Detroit)[42,43] closely follow our seasonal emission estimates including a noticeable summertime Hg(0) increase (**Fig. 4**). Regional background sites in North America however show a consistent summertime minimum (**Fig. 4**), which cannot be explained by anthropogenic Hg emissions, implying that other processes drive the lower Hg(0) levels in summer. Inverse modeling, that optimized terrestrial-atmosphere Hg(0) exchange fluxes to fit observational Hg(0) data, suggested enhanced summertime net Hg(0) deposition over eastern North America[44] supporting the strong role of vegetation as a pump for Hg(0). In Europe and Asia, the anthropogenic Hg(0) emission estimates based on coal consumption data are highest in winter (Table S4) with no summertime increase and a seasonality similar to Hg(0) observations (Fig. 4). Higher Hg(0) concentrations during summer months at urban sites in Asia have been attributed to enhanced re-volatilization of deposited Hg.[45] For the Waldhof site in central Europe, regional models have found a strong

correlation between emission and particulate mercury but not for Hg(0).[46] We therefore conclude that variations in primary anthropogenic emissions alone cannot explain the observed seasonal Hg(0) variation in the NH.

Implications for global Hg cycling

Hg(0) concentrations measured in the PBL at terrestrial background sites reflect both deposition and emission processes. Therefore observed Hg(0) oscillations can be considered as variations in net exchange (vegetation uptake – soil/vegetation re-emission). The strong depletion of atmospheric Hg(0) observed at terrestrial background sites in summer, despite highest solar radiation and therefore potential photo-reductive re-emission, suggests that terrestrial ecosystems are net sinks for Hg(0). We therefore conclude that vegetation uptake of Hg(0) is large and dominates over other terrestrial emission and deposition processes at a regional and global scale. Considering an atmospheric Hg(0) pool of 4800 Mg,[47] the 20% amplitude of seasonal Hg(0) oscillations indicate that terrestrial ecosystems are drawing approximately 1000 Mg a^{-1} of Hg(0) from the atmosphere via the vegetation pump, which is in agreement with foliage/litterfall estimates[17,23]. This suggests that approximately half of the annual primary anthropogenic emissions are assimilated by terrestrial vegetation, where it is efficiently retained against re-emission to the atmosphere, though susceptible to transfer via soils to continental and coastal aquatic ecosystems.[21]

We suggest that the vegetation pump controls to a large extent diurnal and seasonal cycling of atmospheric Hg(0) in the terrestrial PBL, which has large implications for global Hg cycling and interpreting and forecasting long-term trends. The absence of Hg(0) seasonality observed in the SH seems inconsistent with our current understanding of fast Hg(0) oxidation in the atmosphere[7,9,47] A dominant role of plants in NH Hg(0) seasonality may imply that atmospheric Hg(0) oxidation is less important than currently assumed. Average Hg(0) levels in the NH have decreased by 20-40 % between 1990 and 2010 and were recently attributed to a cumulative 30% (≈600 Mg a^{-1}) decrease in global primary anthropogenic Hg(0) emissions.[24] Over the same time period, net primary production (NPP) is thought to have increased in the NH by 0.13-0.15 Pg C a^{-1}.[48,49] Assuming median foliar Hg concentrations of 24 ng g^{-1},[17] we estimate that Hg(0) deposition by NH vegetation uptake today has increased by ≈140 Mg a^{-1} relative to 1990. We therefore suggest that a significant fraction of the observed decrease in NH atmospheric Hg(0) concentrations resulted from increased vegetation uptake of Hg(0). Recent estimates of gross primary production (GPP), based on atmospheric COS

This is a post print version
DOI to the published version in Nature Geoscience: https://doi.org/10.1038/s41561-018-0078-8

cycling, suggested even larger increases in GPP by 31% during the twentieth century[50], that may have strongly counterbalanced estimated increases in Hg(0) emissions. Regional reductions in vegetation cover by deforestation[51] or droughts[49] on the other hand would slow down or cease the vegetation Hg(0) pump, potentially resulting in higher atmospheric Hg(0) concentrations. We therefore emphasize the need to incorporate seasonal and spatial variability in vegetation uptake of Hg(0) into global Hg models to better assess its impact on regional and global Hg cycling. Trends in vegetation cover should be incorporated in models reconstructing past and predicting future Hg(0) levels. The effects of Hg(0) uptake by vegetation related to climate change and land-use change should be considered when discussing mitigation strategies to reduce human Hg exposure. Finally, the paradigm shift we propose regarding the dominant global atmospheric Hg deposition pathway demands revised Hg deposition monitoring strategies by environmental agencies.

This is a post print version
DOI to the published version in Nature Geoscience: https://doi.org/10.1038/s41561-018-0078-8

Data, Materials & Methods

Atmospheric CO_2 and Hg(0) measurements. The focus of the present analysis is on atmospheric monitoring sites that simultaneously measured Hg(0) and CO_2 concentrations. As atmospheric oxidized mercury species account for a minor fraction of total atmospheric Hg (Hg_{tot}) in the PBL, no difference was made between Hg(0) and Hg_{tot} and all data are reported as Hg(0). High resolution QA/QC controlled Hg(0) and CO_2 data were obtained from global air monitoring databases or directly from the responsible site scientists. The European data are harmonised and quality assured following the EMEP program and monitoring strategy, see Tørseth, et al. [52] Hg(0) concentrations at all sites except Pallas were measured at high frequency (5-15 min) using Tekran Continous Mercury Vapor Analyzers 2537 and reported as 1h averages. For Cape Point, SA and Amsterdam Island, Fr all Hg(0) measurements were made in compliance with the GMOS quality assurance protocol (www.gmos.eu). Hg(0) concentrations at Pallas were measured using a semi-automatic sampling on Au-traps (quartz glass coated with gold) at an air sampling rate of 300 ml/min during 24h periods, two days per week. The samples were analyzed on a Tekran 2500 CVAFS Mercury Detector at the IVL laboratory in Gothenburg. CO_2 at Birkenes was measured with Cavity Ringdown spectroscopy (CRDS), Picarro G1301 with 5 s resolution, average to 1 h if data coverage was more than 75%. The data are calibrated against WMO- Global Atmospheric Watch standards at EMPA. CO_2 data from Amsterdam Island, Fr was measured using CRDS and from Egbert, Ca and Cape Point, SA using Non-Dispersive Infrared (NDIR) sensors. CO_2 data from Schauinsland, De were measured by IR-Absorption. All data from Birkenes, No, Amsterdam Island, Fr, Egbert, Ca, Cape Point, SA and Schauinsland, De were measured continuously and reported as hourly averages. CO_2 data from Pallas, Fi and Mace Head, Ir were measured on an event base with flasks and analysed using NDIR.[53] Monthly average Hg(0) data were obtained from.[4,42,43,45,54-58,6,59-61]

Normal Differenced Vegetation Index, (NDVI) were obtained from from the NASA Earth Observations (NEO) platform at 16 days and 0.1° resolution. NDVI data are derived from Moderate Resolution Imaging Spectroradiometer (MODIS) images aboard the NASA's Terra and Aqua satellites.

Statistics

The Co-variance between Hg(0) and CO_2 was assessed using Pearson's product moment correlation coefficient with the cor.test function of the stats (v3.1.3) package and long-term trends of time series as well as linear regression's of Hg(0) and CO2 with NDVI were assessed

This is a post print version
DOI to the published version in Nature Geoscience: https://doi.org/10.1038/s41561-018-0078-8

with the lm function of R.[62] Students t-tests were performed with Microsoft Excel assuming uneven variances.

Seasonality of anthropogenic Hg emission. The monthly Hg emission for the different regions ($F(Hg)_{month}$) in Mg Hg/month was calculated according to Formula 1:

$$F(Hg)_{month} = f_{coal} * f_{consumption} * FHg_{year} + (1 - f_{coal}) * {}^{1}/_{12} * FHg_{year} \quad (1)$$

where f_{coal} and $F(Hg)_{year}$ corresponds to the fraction of Hg emission based on coal combustion and the total yearly Hg emission for each investigated country, based on the AMAP/UNEP 2010 mercury emission estimates[63]. $f_{consumption}$ corresponds to the monthly fraction of the yearly coal consumption. For the USA and Europe (27 EU countries) monthly coal consumption data are reported by governmental agencies. Seasonality of Hg emission from China was derived from the monthly power generation data between 2005 and 2010 reported by Liu et al. 2015[64]. The monthly cement production in China was considered constant throughout the year[65].

Normalization of monthly Hg concentration and emission data. In Figure 1 monthly Hg concentrations and emission fluxes are normalized to yearly averages for comparability. Hg concentrations are normalized as follows: $C(Hg0)_{monthx}$ /$C(Hg0)_{year,}$ were $C(Hg0)_{monthx}$ represents the multiyear monthly average of month x and $C(Hg0)_{year}$ the yearly average.

Computation of Seasonal Amplitudes. The absolute seasonal amplitudes are calculated from the multiyear monthly averages as follows: (μM_{max} - μM_{min}), were μM_{max} and μM_{min} represent the averages of the months with NH maximum (February for both Hg(0) and CO_2) and minimum (August for CO_2 and September for Hg(0)) concentration (Table S6-S10), respectively. Relative amplitudes are calculated as follows: (μM_{max} - μM_{min})/ μY, were μY represents the yearly average.

Data availability

Most European Hg(0) data used are associated to EMEP, and publically available through the EMEP data base, EBAS: http://ebas.nilu.no. CO2 concentrations were obtained from the ESRL NOAA Global Monitoring Division database (ftp://aftp.cmdl.noaa.gov/data/trace_gases/co2/flask/surface/co2_mhd_surface-flask_1_ccgg_event.txt, ftp://aftp.cmdl.noaa.gov/data/trace_gases/co2/flask/surface/co2_pal_surface-flask_1_ccgg_event.txt) and the World Data Center for Greenhouse Gases WDCGG (http://ds.data.jma.go.jp/gmd/wdcgg/). Canadian Hg(0) concentrations were obtained from

the National Atmospheric Chemistry (NAtChem) Database and Analysis Facility of Environment Canada (www.ec.gc.ca/natchem).

For the USA and Europe (27 EU countries) monthly coal consumption are reported by the U.S. Energy Information Administration (http://www.eia.gov/totalenergy, downloaded 25.5.2016) and Eurostat (http://ec.europa.eu/eurostat/statistics-explained/index.php/Coal_consumption_statistics, downloaded 15.2.2016), respectively. NDVI data was obtained from the NASA Earth Observations (NEO) platform (http://neo.sci.gsfc.nasa.gov)

Acknowledgement

We thank those who are involved in the EMEP efforts and have contributed through operating sites, performing chemical analysis and by submissions of data to the data base EBAS. EMEP is funded through national contributions. We gratefully acknowledge the Air Quality Research Division of Environment Canada for the Total Gaseous Mercury data and the ESRL NOAA and WDCGG data centers for the CO_2 data. This work was also funded by H2020 Marie Sklodowska-Curie grant agreement No 657195 to MJ, European Research Council grant ERC-2010-StG_20091028 and CNRS-INSU-CAF funding (PARCS project) to JES.

Author Contribution

MJ initiated the project, performed the data analysis and wrote the manuscript together with JES and contributions from DO, JB and AD. JB, RE, CML, KA, IW, KK, DW, LM, CL, TM, MR, OM, and AD provided data. All Authors read and commented on the manuscript.

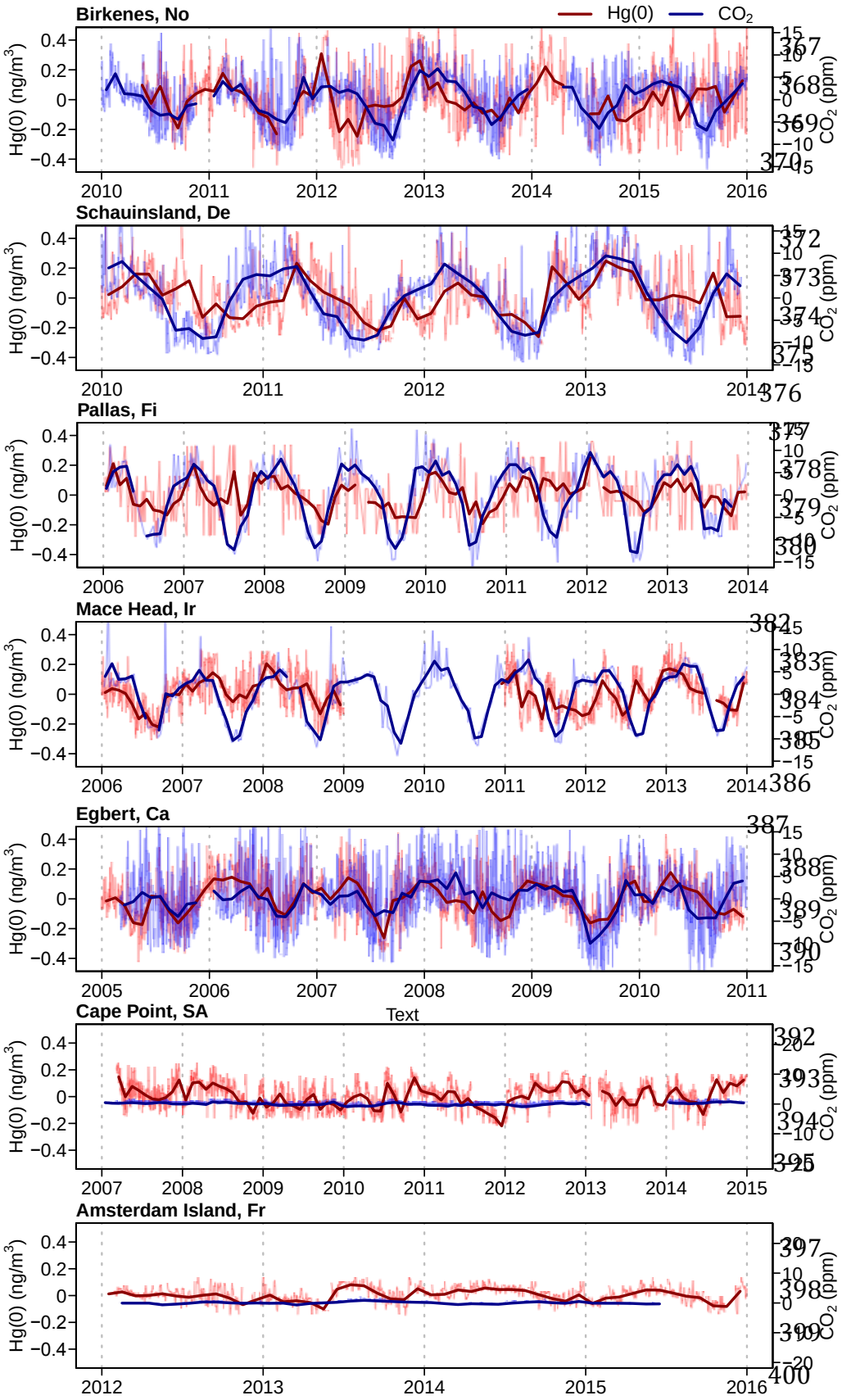

Fig. 1: Seasonal oscillations of atmospheric Hg(0) (red) and CO_2 (blue) concentration at several monitoring sites around the globe. Fine lines represent daily and bold lines represent monthly

This is a post print version
DOI to the published version in Nature Geoscience: https://doi.org/10.1038/s41561-018-0078-8

anomalies normalized for long-term linear trends. All data meeting QA/QC criteria of the respective site are presented.

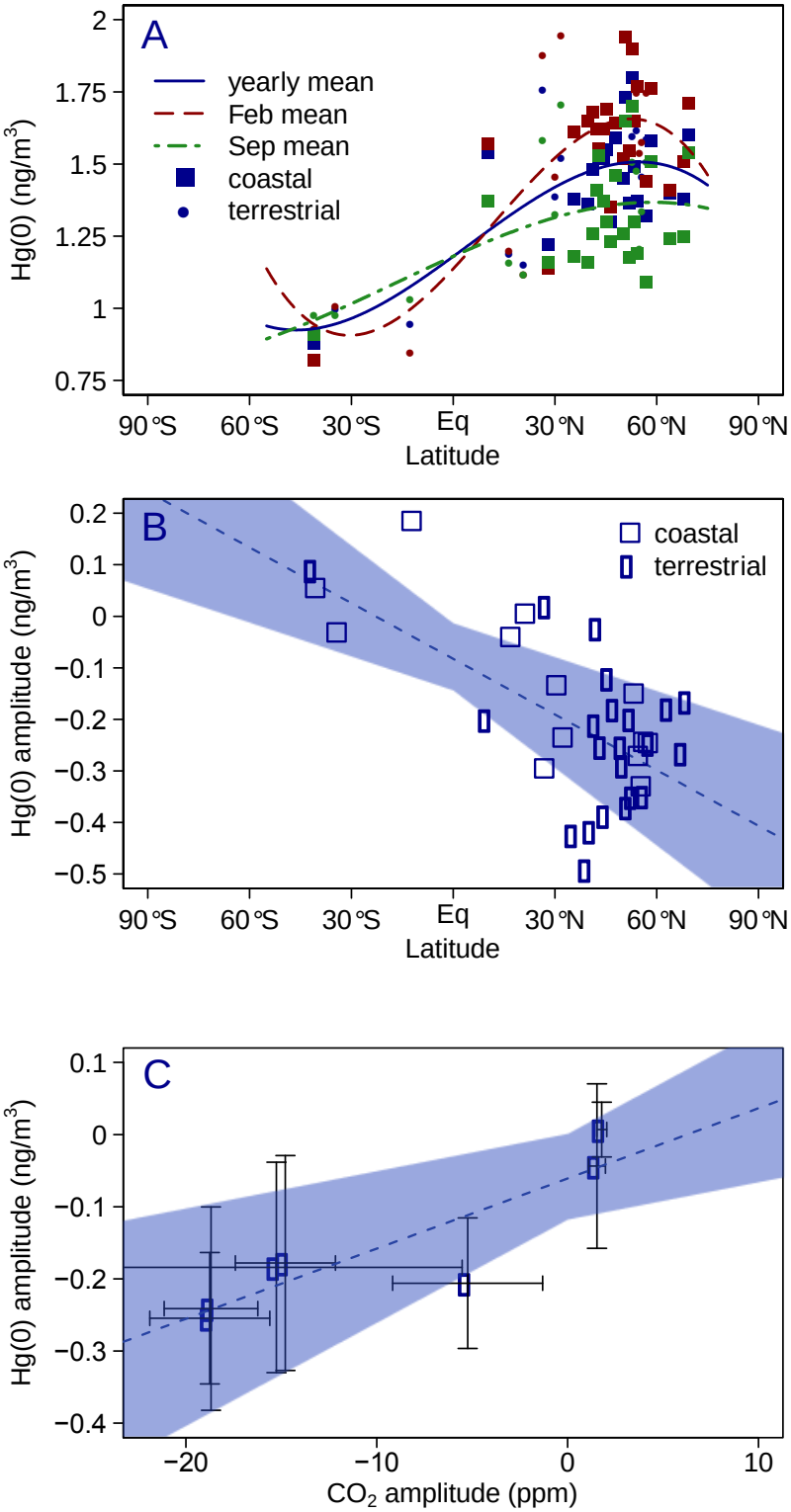

Fig. 2: A: Interhemispherical Gradient of Hg(0) at background sites (<2 ng/m³). The lines represent polynomial fits of the measurements for the yearly mean and the monthly means of February and September. B: Seasonal amplitude of Hg(0) (September mean - February mean) as a function of latitude for coastal (squares) and terrestrial (circles) sites. The dashed line

This is a post print version
DOI to the published version in Nature Geoscience: https://doi.org/10.1038/s41561-018-0078-8

represents the linear fit of the data and the shaded area the 95% confidence area. C: Seasonal amplitudes of Hg(0) (Sep-Feb) and CO_2 (Aug-Feb) variation measured at 7 atmospheric sites. The error bars represent the interannual variability (1σ). The dashed line represents the linear fit of the data and the shaded area the 95% confidence area.

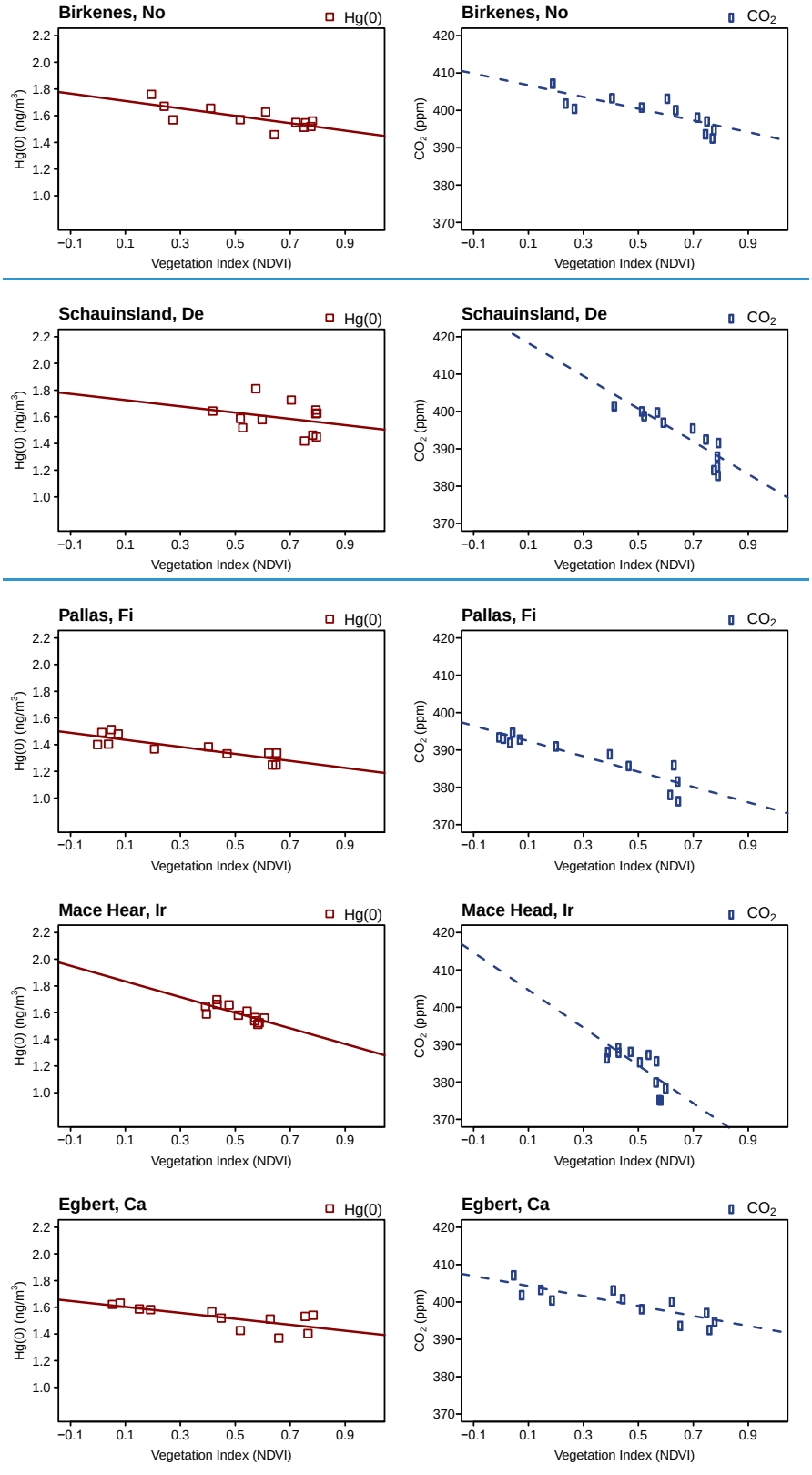

This is a post print version
DOI to the published version in Nature Geoscience: https://doi.org/10.1038/s41561-018-0078-8

Figure 2: Linear correlation between multi-year averages of monthly Hg(0) concentration and NDVI (left) and CO_2 concentration and NDVI (right) at five NH monitoring stations.

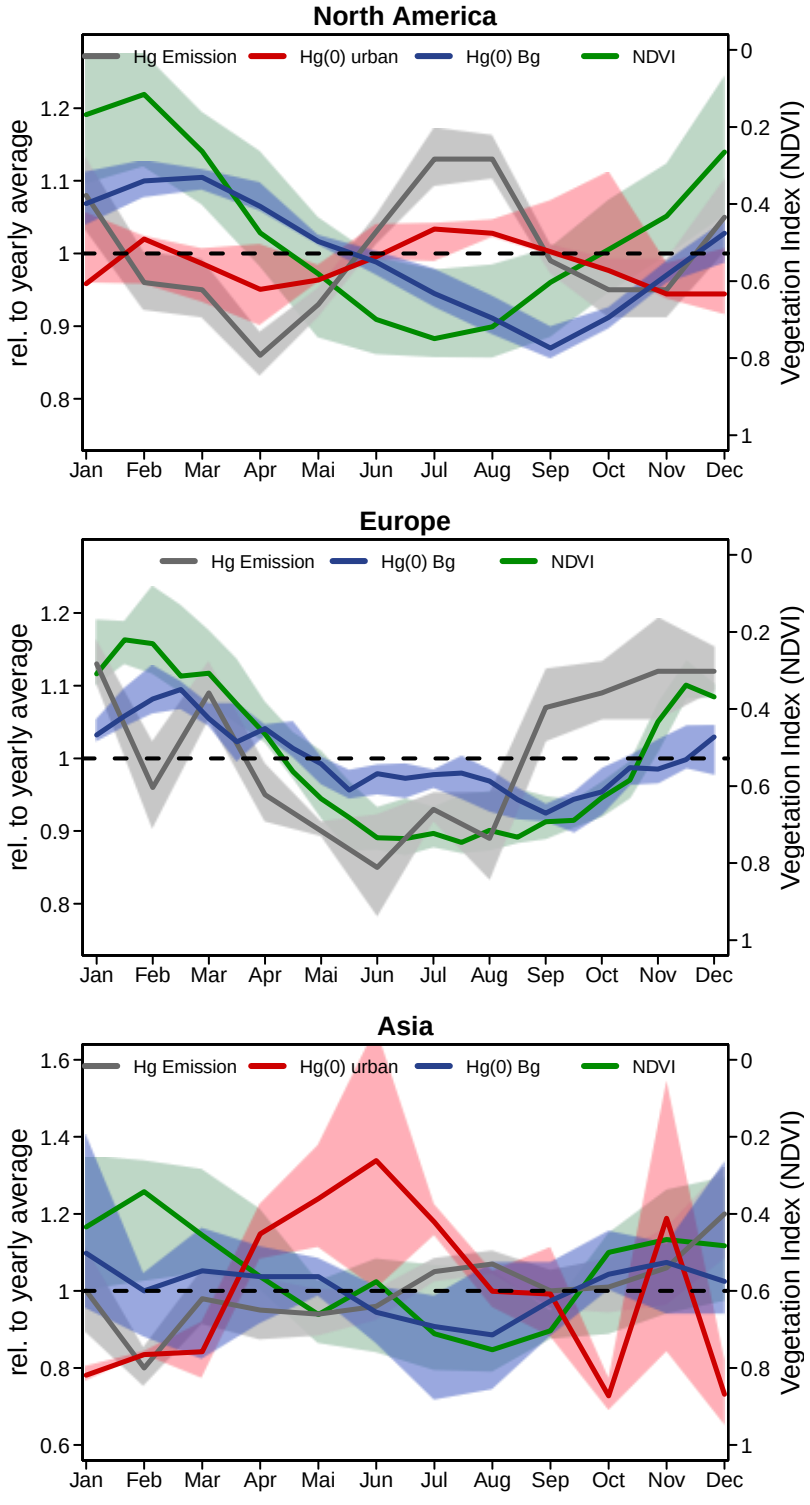

Fig. 4: Seasonal variation of Hg emissions in gray, atmospheric Hg(0) concentration at terrestrial background sites (Hg(0) Bg) in blue and at urban sites (Hg(0) urban) in red and Vegetation index (NDVI) in green. Monthly Hg emission and Hg(0) concentrations are reported

This is a post print version
DOI to the published version in Nature Geoscience: https://doi.org/10.1038/s41561-018-0078-8

relative to yearly average. The bold lines represent averages and the shaded areas represent 25th to 75th percentiles.

References

1 Krabbenhoft, D. P. & Sunderland, E. M. Global Change and Mercury. *Science* **341**, 1457-1458, doi:10.1126/science.1242838 (2013).

2 Driscoll, C. T., Mason, R. P., Chan, H. M., Jacob, D. J. & Pirrone, N. Mercury as a global pollutant: sources, pathways, and effects. *Environ. Sci. Technol.* **47**, 4967-4983, doi:10.1021/es305071v (2013).

3 Temme, C. *et al.* Trend, seasonal and multivariate analysis study of total gaseous mercury data from the Canadian atmospheric mercury measurement network (CAMNet). *Atmospheric Environment* **41**, 5423-5441, doi:http://dx.doi.org/10.1016/j.atmosenv.2007.02.021 (2007).

4 Fu, X. W. *et al.* Observations of atmospheric mercury in China: a critical review. *Atmos. Chem. Phys.* **15**, 9455-9476, doi:10.5194/acp-15-9455-2015 (2015).

5 Weigelt, A. *et al.* Analysis and interpretation of 18 years of mercury observations since 1996 at Mace Head, Ireland. *Atmospheric Environment* **100**, 85-93, doi:10.1016/j.atmosenv.2014.10.050 (2015).

6 Sprovieri, F. *et al.* Atmospheric Mercury Concentrations observed at ground-based monitoring sites globally distributed in the framework of the GMOS network. *Atmos. Chem. Phys. Discuss.* **2016**, 1-32, doi:10.5194/acp-2016-466 (2016).

7 Holmes, C. D. *et al.* Global atmospheric model for mercury including oxidation by bromine atoms. *Atmos. Chem. Phys.* **10**, 12037-12057, doi:10.5194/acp-10-12037-2010 (2010).

8 Song, S. *et al.* Top-down constraints on atmospheric mercury emissions and implications for global biogeochemical cycling. *Atmos. Chem. Phys.* **15**, 7103-7125, doi:10.5194/acp-15-7103-2015 (2015).

9 Horowitz, H. M. *et al.* A new mechanism for atmospheric mercury redox chemistry: Implications for the global mercury budget. *Atmos. Chem. Phys. Discuss.* **2017**, 1-33, doi:10.5194/acp-2016-1165 (2017).

10 Selin, N. E. *et al.* Chemical cycling and deposition of atmospheric mercury: Global constraints from observations. *J. Geophys. Res.-Atmos.* **112**, doi:D02308 10.1029/2006jd007450 (2007).

11 Slemr, F. *et al.* Comparison of mercury concentrations measured at several sites in the Southern Hemisphere. *Atmos. Chem. Phys.* **15**, 3125-3133, doi:10.5194/acp-15-3125-2015 (2015).

12 Khalil, M. A. K. & Rasmussen, R. A. Sources, sinks, and seasonal cycles of atmospheric methane. *Journal of Geophysical Research: Oceans* **88**, 5131-5144, doi:10.1029/JC088iC09p05131 (1983).

13 Rea, A. W., Lindberg, S. E., Scherbatskoy, T. & Keeler, G. J. Mercury accumulation in foliage over time in two northern mixed-hardwood forests. *Water Air Soil Pollut.* **133**, 49-67, doi:10.1023/a:1012919731598 (2002).

14 St Louis, V. L. *et al.* Importance of the forest canopy to fluxes of methyl mercury and total mercury to boreal ecosystems. *Environ. Sci. Technol.* **35**, 3089-3098, doi:10.1021/es001924p (2001).

15 Lindberg, S. *et al.* A Synthesis of Progress and Uncertainties in Attributing the Sources of Mercury in Deposition. *Ambio* **36**, 19-32 (2007).

16 Smith-Downey, N. V., Sunderland, E. M. & Jacob, D. J. Anthropogenic impacts on global storage and emissions of mercury from terrestrial soils: Insights from a new global model. *J. Geophys. Res.-Biogeosci.* **115**, doi:10.1029/2009jg001124 (2010).

17 Obrist, D. Atmospheric mercury pollution due to losses of terrestrial carbon pools? *Biogeochemistry* **85**, 119-123, doi:10.1007/s10533-007-9108-0 (2007).

18 Amos, H. M., Jacob, D. J., Streets, D. G. & Sunderland, E. M. Legacy impacts of all-time anthropogenic emissions on the global mercury cycle. *Global Biogeochem. Cycles* **27**, 410-421, doi:10.1002/gbc.20040 (2013).

19 Agnan, Y., Le Dantec, T., Moore, C. W., Edwards, G. C. & Obrist, D. New Constraints on Terrestrial Surface-Atmosphere Fluxes of Gaseous Elemental Mercury Using a Global Database. *Environ Sci Technol* **50**, 507-524, doi:10.1021/acs.est.5b04013 (2016).

20 Laacouri, A., Nater, E. A. & Kolka, R. K. Distribution and Uptake Dynamics of Mercury in Leaves of Common Deciduous Tree Species in Minnesota, U.S.A. *Environmental Science & Technology* **47**, 10462-10470, doi:10.1021/es401357z (2013).

21 Obrist, D. *et al.* Tundra uptake of atmospheric elemental mercury drives Arctic mercury pollution. *Nature* **547**, 201-204, doi:10.1038/nature22997(2017).

22 Graydon, J. A., St. Louis, V. L., Lindberg, S. E., Hintelmann, H. & Krabbenhoft, D. P. Investigation of Mercury Exchange between Forest Canopy Vegetation and the Atmosphere Using a New Dynamic Chamber†. *Environmental Science & Technology* **40**, 4680-4688, doi:10.1021/es0604616 (2006).

23 Wang, X., Bao, Z., Lin, C. J., Yuan, W. & Feng, X. Assessment of Global Mercury Deposition through Litterfall. *Environ Sci Technol* **50**, 8548-8557, doi:10.1021/acs.est.5b06351 (2016).

24 Zhang, Y. *et al.* Observed decrease in atmospheric mercury explained by global decline in anthropogenic emissions. *Proceedings of the National Academy of Sciences*, doi:10.1073/pnas.1516312113 (2016).

25 Demers, J. D., Blum, J. D. & Zak, D. R. Mercury isotopes in a forested ecosystem: Implications for air-surface exchange dynamics and the global mercury cycle. *Global Biogeochem. Cycles* **27**, 222-238, doi:Doi 10.1002/Gbc.20021 (2013).

26 Enrico, M. *et al.* Atmospheric mercury transfer to peat bogs dominated by gaseous elemental mercury dry deposition. *Environ Sci Technol* **50**, 2405-2412, doi:10.1021/acs.est.5b06058 (2016).

27 Jiskra, M. *et al.* Mercury deposition and re-emission pathways in boreal forest soils investigated with Hg isotope signatures. *Environ Sci Technol* **49**, 7188-7196, doi:10.1021/acs.est.5b00742 (2015).

28 Keeling, C. D. *et al.* Atmospheric carbon dioxide variations at Manua-Lao observatory, Hawaii. *Tellus* **28**, 538-551 (1976).

29 Keeling, C. D., Chin, J. F. S. & Whorf, T. P. Increased activity of northern vegetation inferred from atmospheric CO2 measurements. *Nature* **382**, 146-149, doi:10.1038/382146a0 (1996).

30 Denning, A. S., Fung, I. Y. & Randall, D. Latitudinal gradient of atmospheric CO2 due to seasonal exchange with land biota. *Nature* **376**, 240-243 (1995).

31 UNEP. Global Mercury Assessment 2013: Sources, Emissions, Releases and Environmental Tramsport. (UNEP Chemicals Branch, Geneva, Switzerland, 2013).

32 Steffen, A. *et al.* A synthesis of atmospheric mercury depletion event chemistry in the atmosphere and snow. *Atmospheric Chemistry and Physics* **8**, 1445-1482 (2008).

33 Diéguez, M. C. *et al.* Four years of atmospheric mercury records in Northwestern Patagonia (Argentina): potential sources, concentration patterns and influence of environmental variables observed at the GMOS EMMA station. *Atmos. Chem. Phys. Discuss.* **2017**, 1-18, doi:10.5194/acp-2016-1076 (2017).

34 Fritsche, J. *et al.* Elemental mercury fluxes over a sub-alpine grassland determined with two micrometeorological methods. *Atmospheric Environment* **42**, 2922-2933, doi:DOI 10.1016/j.atmosenv.2007.12.055 (2008).

35 Poissant, L., Pilote, M., Yumvihoze, E. & Lean, D. Mercury concentrations and foliage/atmosphere fluxes in a maple forest ecosystem in Québec, Canada. *Journal of Geophysical Research* **113**, n/a-n/a, doi:10.1029/2007jd009510 (2008).

36 Fu, X. *et al.* Depletion of atmospheric gaseous elemental mercury by plant uptake at Mt. Changbai, Northeast China. *Atmos. Chem. Phys. Discuss.* **2016**, 1-31, doi:10.5194/acp-2016-391 (2016).

37 Wofsy, S. C. *et al.* (Science, 1993).

38 Commane, R. *et al.* Seasonal fluxes of carbonyl sulfide in a midlatitude forest. *Proceedings of the National Academy of Sciences* **112**, 14162-14167, doi:10.1073/pnas.1504131112 (2015).

39 Wehr, R. *et al.* Dynamics of canopy stomatal conductance, transpiration, and evaporation in a temperate deciduous forest, validated by carbonyl sulfide uptake. *Biogeosciences* **14**, 389-401, doi:10.5194/bg-14-389-2017 (2017).

40 Obrist, D. *et al.* A synthesis of terrestrial mercury in the western United States: Spatial distribution defined by land cover and plant productivity. *Sci Total Environ* **568**, 522-535, doi:10.1016/j.scitotenv.2015.11.104 (2016).

41 Blasing, T. J., Broniak, C. T. & Marland, G. The annual cycle of fossil-fuel carbon dioxide emissions in the United States. *Tellus B* **57**, doi:10.3402/tellusb.v57i2.16779 (2011).

42 Lan, X., Talbot, R., Castro, M., Perry, K. & Luke, W. Seasonal and diurnal variations of atmospheric mercury across the US determined from AMNet monitoring data. *Atmospheric Chemistry and Physics* **12**, 10569-10582, doi:10.5194/acp-12-10569-2012 (2012).

43 Xu, X. H., Akhtar, U., Clark, K. & Wang, X. B. Temporal Variability of Atmospheric Total Gaseous Mercury in Windsor, ON, Canada. *Atmosphere* **5**, 536-556, doi:10.3390/atmos5030536 (2014).

44 Song, S. *et al.* Constraints from observations and modeling on atmosphere–surface exchange of mercury in eastern North America. *Elementa: Science of the Anthroposcene* **4**, doi:10.12952/journal.elementa.000100 (2016).

45 Zhu, J. *et al.* Characteristics of atmospheric Total Gaseous Mercury (TGM) observed in urban Nanjing, China. *Atmospheric Chemistry and Physics* **12**, 12103-12118, doi:10.5194/acp-12-12103-2012 (2012).

46 Bieser, J. *et al.* in *Air Pollution Modeling and its Application XXIII* (eds Douw Steyn & Rohit Mathur) 189-195 (Springer International Publishing, 2014).

47 Bieser, J. *et al.* Multi-model study of mercury dispersion in the atmosphere: Vertical distribution of mercury species. *Atmos. Chem. Phys. Discuss.* **2016**, 1-54, doi:10.5194/acp-2016-1074 (2016).

48 Nemani, R. R. *et al.* Climate-Driven Increases in Global Terrestrial Net Primary Production from 1982 to 1999. *Science* **300**, 1560-1563, doi:10.1126/science.1082750 (2003).

49 Zhao, M. & Running, S. W. Drought-Induced Reduction in Global Terrestrial Net Primary Production from 2000 Through 2009. *Science* **329**, 940 (2010).

50 Campbell, J. E. *et al.* Large historical growth in global terrestrial gross primary production. *Nature* **544**, 84-87, doi:10.1038/nature22030

51 Baccini, A. *et al.* Estimated carbon dioxide emissions from tropical deforestation improved by carbon-density maps. *Nature Clim. Change* **2**, 182-185, doi:http://www.nature.com/nclimate/journal/v2/n3/abs/nclimate1354.html#supplementary-information (2012).

52 Tørseth, K. *et al.* Introduction to the European Monitoring and Evaluation Programme (EMEP) and observed atmospheric composition change during 1972-2009. *Atmos. Chem. Phys.* **12**, 5447-5481, doi:10.5194/acp-12-5447-2012 (2012).

53 Dlugokencky, E. J., P.M. Lang, J.W. Mund, A.M. Crotwell, & M.J. Crotwell, a. K. W. T. *Atmospheric Carbon Dioxide Dry Air Mole Fractions from the NOAA ESRL Carbon Cycle Cooperative Global Air Sampling Network, 1968-2015*, <ftp://aftp.cmdl.noaa.gov/data/trace_gases/co2/flask/surface/> (2016).

54 Jiang, Y., Cizdziel, J. V. & Lu, D. Temporal patterns of atmospheric mercury species in northern Mississippi during 2011–2012: Influence of sudden population swings. *Chemosphere* **93**, 1694-1700, doi:http://dx.doi.org/10.1016/j.chemosphere.2013.05.039 (2013).

55 Lan, X. *et al.* Seasonal and Diurnal Variations of Total Gaseous Mercury in Urban Houston, TX, USA. *Atmosphere* **5**, 399-419, doi:10.3390/atmos5020399 (2014).

56 Cole, A. *et al.* A Survey of Mercury in Air and Precipitation across Canada: Patterns and Trends. *Atmosphere* **5**, 635 (2014).

57 Sheu, G. R. *et al.* Temporal distribution and potential sources of atmospheric mercury measured at a high-elevation background station in Taiwan. *Atmospheric Environment* **44**, 2393-2400, doi:10.1016/j.atmosenv.2010.04.009 (2010).

This is a post print version
DOI to the published version in Nature Geoscience: https://doi.org/10.1038/s41561-018-0078-8

58 Zhang, L., Wang, S. X., Wang, L. & Hao, J. M. Atmospheric mercury concentration and chemical speciation at a rural site in Beijing, China: implications of mercury emission sources. *Atmospheric Chemistry and Physics* **13**, 10505-10516, doi:10.5194/acp-13-10505-2013 (2013).

59 Read, K. A. *et al.* Four years (2011–2015) of total gaseous mercury measurements from the Cape Verde Atmospheric Observatory. *Atmos. Chem. Phys.* **17**, 5393-5406, doi:10.5194/acp-17-5393-2017 (2017).

60 Denzler, B. *et al.* Inversion Approach to Validate Mercury Emissions Based on Background Air Monitoring at the High Altitude Research Station Jungfraujoch (3580 m). *Environmental Science & Technology* **51**, 2846-2853, doi:10.1021/acs.est.6b05630 (2017).

61 Howard, D. *et al.* Atmospheric mercury in the southern hemisphere tropics: seasonal and diurnal variations and influence of inter-hemispheric transport. *Atmos. Chem. Phys. Discuss.* **2017**, 1-20, doi:10.5194/acp-2017-307 (2017).

62 R: A Language and Environment for Statistical Computing (Vienna, Austria, 2015).

63 AMAP/UNEP. Technical Background Report for Global Mercury assessment 2013. (UNEP Chemical Branch, Geneva, Switzerland, 2013).

64 Liu, F. *et al.* High-resolution inventory of technologies, activities, and emissions of coal-fired power plants in China from 1990 to 2010. *Atmos. Chem. Phys.* **15**, 13299-13317, doi:10.5194/acp-15-13299-2015 (2015).

65 Zhu, J., Wang, T., Bieser, J. & Matthias, V. Source attribution and process analysis for atmospheric mercury in eastern China simulated by CMAQ-Hg. *Atmos. Chem. Phys.* **15**, 8767-8779, doi:10.5194/acp-15-8767-2015 (2015).